CERN - European Organization for Nuclear Research

LCD-Note-2011-002

The CLIC_ILD_CDR Geometry for the CDR Monte Carlo Mass Production

A. Münnich *, A. Sailer* †

* *CERN, Switzerland,* † *Humboldt-Universität zu Berlin, Germany*

Version 7, November 25, 2014

Abstract

The CLIC_ILD_CDR detector for the Monte Carlo event simulation is described in a GEANT4 application, with some parameters available in a database and XML files. This makes it difficult to quickly "look up" interesting parameters of the detector geometry used for the simulation. This note summarises the important geometrical parameters and some details of the implemented detector components.

1. Introduction

This note describes the CLIC_ILD_CDR detector model used for the CLIC Conceptual Design Report (CDR). The detector is described as implemented in the Monte Carlo simulation.

The next section provides an overview of the CLIC_ILD_CDR geometry. The different detector subsystems are described in more detail in the latter sections. In Section 3 the detectors used for tracking and vertexing and in Subsection 4.2 the calorimeter and muon systems are described. The coil and magnetic field used for the simulation is briefly described in Section 5. Descriptions of the very forward region calorimeters and accelerator components inside the detector can be found in Section 6. The last section (7) gives some details on the simulation software and parameters used for the simulation.

2. CLIC_ILD_CDR Overview

The CLIC_ILD_CDR detector model is based on the ILD detector model [1] designed for the ILC. Like every good 4π general purpose detector it is built like the layers of an onion. Unlike most of its predecessors, but like its ILC counterpart, the CLIC_ILD detector is developed with the Particle Flow (PF) paradigm in mind. Figure 1 shows a quadrant of the CLIC_ILD_CDR detector and Table 1 presents the general parameters for the detector model. Overall the detector is 14 m long and has a diameter of 14 m (from flat to flat side of the dodecagonal cross section).

The detector consists of a silicon based Vertex Detector (VXD) and Forward Tracking Disks (FTDs). In the central region the VXD is followed by the Silicon Internal Tracker (SIT). The inner silicon based tracking is followed by a Time Projection Chamber (TPC). There are additional silicon sensors beyond the TPC endplate, the Endcap Tracking Disks (ETDs), and around the barrel the Silicon External Tracker (SET).

The tracking system is followed by a silicon-tungsten (SiW) Electromagnetic Calorimeter (ECal) and a scintillator based Hadronic Calorimeter (HCal). The absorber in the barrel of the HCal is tungsten, to obtain a more compact calorimeter, and iron in the endcap, where space is less critical. The calorimeter barrel is surrounded by a superconducting solenoid coil, which provides a 4 T magnetic field. The magnetic flux is contained by an iron return yoke, that is also equipped with layers for muon ID.

In the forward region the coverage of the ECal is complemented by the Luminosity Calorimeter (LumiCal) and the Beam Calorimeter (BeamCal). Figure 2 shows the placement of LumiCal and BeamCal around the beam pipe. The layout of the forward region is dominated by the position and size of the final focus quadrupole (QD0), which is aligned with the endcap of the return yoke. The very forward region is shown in Figure 8.

3. Vertex and Tracking Detectors

The tracking in the CLIC_ILD_CDR detector model consists of silicon based vertex detectors and a time projection chamber as the main central tracking detector. The TPC is surrounded by a silicon envelope. For shallow tracks, that do not pass a significant fraction of the TPC, forward-tracking disks are foreseen.

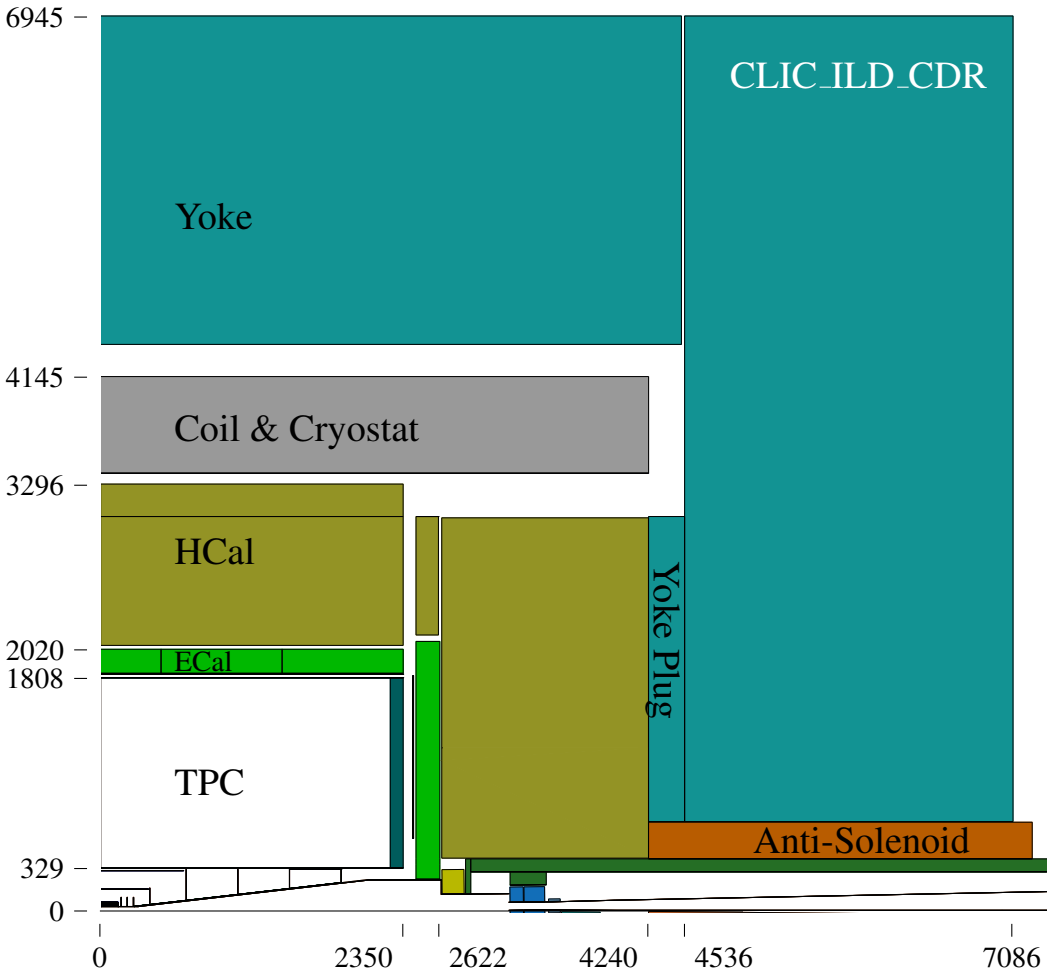

Figure 1: Dimensions of the CLIC_ILD_CDR model as implemented for the simulation. All values are given in millimetre and correspond to Table 1.

3.1. Vertex Detector

The vertex detector (VXD) consists of three double layers. Their position is shown in Figure 3, which also shows the double layer forward-tracking disks. The geometrical parameters for the layers are given in Table 2.

In the current simulation each double layer is represented by two single layers (see Figure 3b). Seen from the interaction point, the inner ladders of each double layer start with the 50 µm thick silicon sensor, which is followed by a support of 67 µm carbon. The outer ladders in each double layer start with the carbon support followed by the silicon. The distance between the inner and outer ladder is 2 mm. For the actual construction of the double layers, it is foreseen that each of the two active layers is mounted on either side of a single support structure, with the same material budget as implemented in the current simulation model (0.18% X_0 per double layer). Finally all layers are supported by a 0.5 mm beryllium scaffold surrounding the vertex detector.

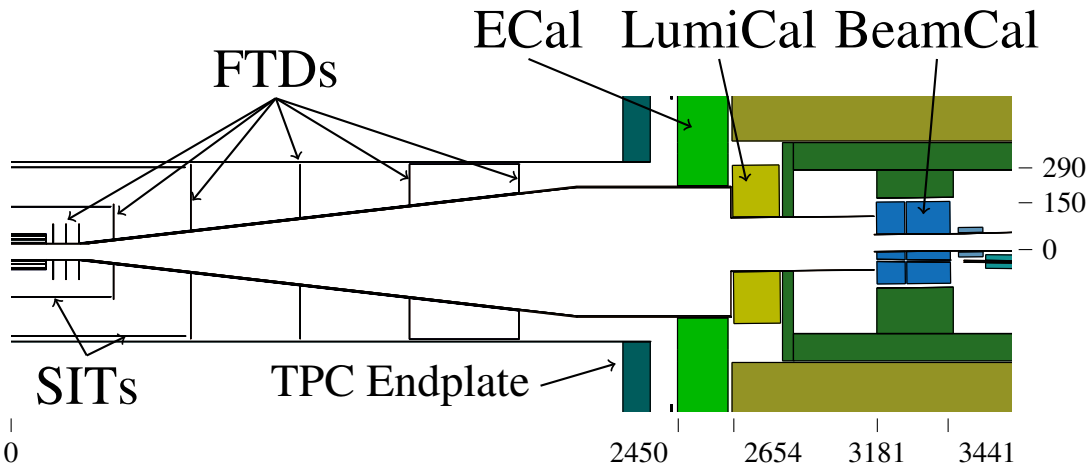

Figure 2: Forward Tracking and Calorimeters seen from the top. The overlap in coverage between LumiCal and ECal is visible. LumiCal and BeamCal look slightly skewed, because they are centred on the outgoing beam axis.

Table 1: General parameters for the CLIC_ILD_CDR detector model. $Z_{\text{Start/End}}$ are the beginning and end in one half of the detector. The parameters $R_{\text{In/Out}}$ are the radii of the inscribing circles for the polygons given in the last column. The polygon column gives the number of corners of the inner and outer polygon.

	Z_{Start} [mm]	Z_{End} [mm]	R_{In} [mm]	R_{Out} [mm]	Polygon[A]	
TPC	0	2350	329	1808	0	0
ECal Barrel	0	2350	1847	2020	8	8
HCal Barrel	0	2350	2058	3296	8	16
Coil	0	4256	3395	4145	0	0
Yoke Barrel	0	4511	4395	6945	12	12
ECal Endcap[B]	2450	2622	242	2089	0	8
HCal Ring	2450	2609	2139	3059	8	8
HCal Endcap	2650	4240	400	3059	4	8
Yoke Plug	4256	4536	690	3059	0	12
Yoke Endcap	4536	7086	690	6945	0	12
LumiCal[C]	2654	2825	100	290	0	0
BeamCal[C]	3181[D]	3441	32	150	0	0

[A] Circles are indicated by “0”, squares by “4”, etc.
[B] The ECal endcap includes the ECal endcap plug.
[C] LumiCal and BeamCal are centred on the outgoing beam axis.
[D] This includes 100 mm of graphite before BeamCal (see Subsection 6.2).

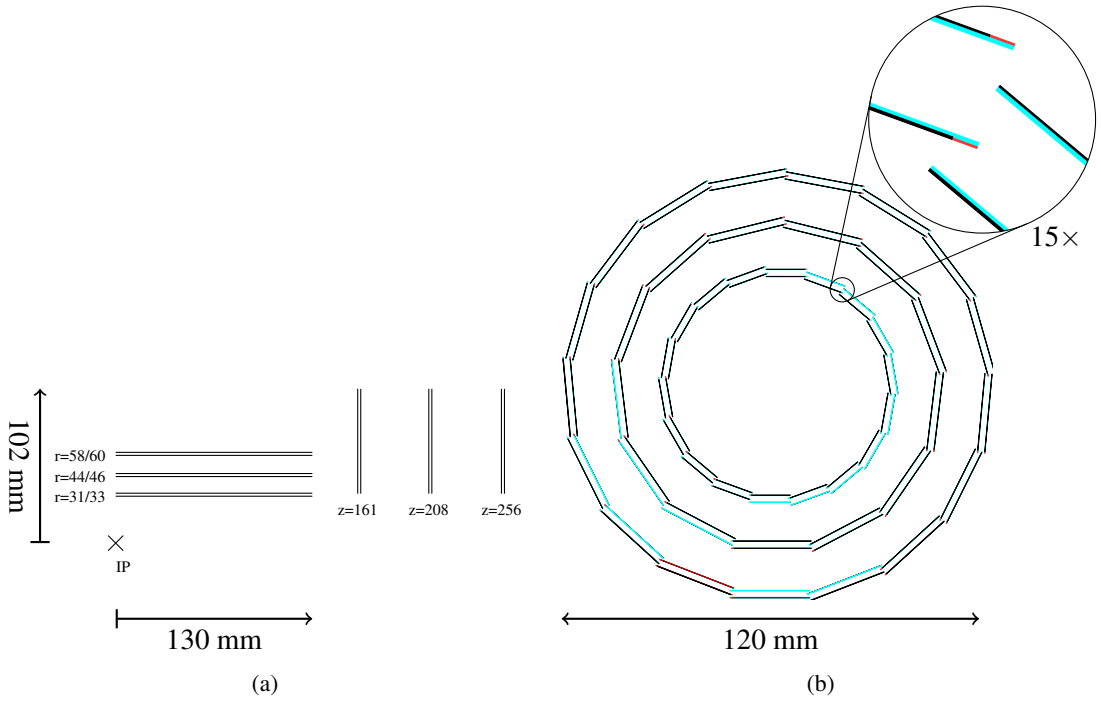

Figure 3: (a) Sketch showing the position of the vertex detector barrel layers and endcap disks. (b) Ladder positions around the beam pipe. The inset region shows the structure of the ladder: The sensor in black, the carbon support in cyan and the readout electronics on the side of the ladders in red.

Table 2: Parameters for the vertex detector barrel layers. The number of ladders N_{Ladder}, the radius R, the half-length l_{Ladder} and width w_{Ladder} of the ladders, the thickness of the active silicon layers d_{Si} and of the support d_{Sup} is given.

Layer	N_{Ladder}	R [mm]	l_{Ladder} [mm]	w_{Ladder} [mm]	d_{Si} [µm]	d_{Sup} [µm]
1	18	31.000	130.0	11.5	50	67
2	18	32.933	130.0	11.5	50	67
3	13	44.000	130.0	22.5	50	67
4	13	45.933	130.0	22.5	50	67
5	17	58.000	130.0	22.5	50	67
6	17	59.933	130.0	22.5	50	67

3.2. Forward Tracking Disks

The six first forward tracking disks act as vertex endcap disks. They are arranged in pairs, like the three double layers of the vertex detector. During the digitization and reconstruction the hits recorded in these disks are considered to come from pixel sensors and treated accordingly, the

hits from the other disks are treated as coming from silicon strip sensors. The position of the innermost FTDs with respect to the vertex barrel can be seen in Figure 3a. The dimensions for all FTDs can be found in Table 3.

Table 3: Vertex- and forward-tracking disk parameters. The inner R_{In} and outer radius R_{Out} and the position in Z is given along with the thickness of the silicon d_{Si} and support d_{Sup}.

Disk	R_{In} [mm]	R_{Out} [mm]	Z [mm]	d_{Si} [µm]	d_{Sup} [µm]
1^{A}	33	102	160	50	76
2^{A}	33	102	162	50	76
3^{A}	33	102	207	50	76
4^{A}	33	102	209	50	76
5^{A}	33	102	255	50	76
6^{A}	33	102	257	50	76
7^{B}	47	175	382	275	1136
8^{B}	79	320	665	275	1136
9^{B}	126	320	1066	275	1136
10^{B}	172	320	1467	275	1136
11^{B}	218	320	1868	275	1136

[A] Digitized as pixel sensors
[B] Digitized as strip Sensors

3.3. Silicon Internal Tracker (SIT)

Two barrel layers of the silicon strips, the so-called Silicon Internal Tracker (SIT), are placed between the VXD barrel layers and the TPC inner radius. The SIT covers an angular region down to 30° (see Figure 6) similar to the range where tracks are passing through the full radius of the TPC. The geometrical parameters for the SIT layers are given in Table 4.

3.4. Time Projection Chamber (TPC)

The TPC is the central tracking device in the ILD detector concept, with an inner radius of 0.33 m, an outer radius of 1.8 m and a half-length of 2.3 m (see Table 5 for all dimensions). It covers tracks down to a polar angle of about 20° to 30° (see Figure 6).

The central cathode of the TPC is a thin sheet of mylar with copper on each side (see Figure 4). The gas is 95.67% argon mixed with 2.27% CO_2 and 2.07% CH_4. In the simulation, the endplate is constructed out of several thin layers of different materials totalling 28% of a radiation length. The field cage is represented by thin aluminium barrels. The inner field cage is 1.16 mm and the outer 1.51 mm thick.

Table 4: Parameters for the silicon envelope of the TPC. R_{In} denotes the inner radius for the ETDs and the cylinder radius for SITs and SETs. R_{Out} is the outer radius of the ETDs. Z is the position of the ETDs and the half-length for the SIT and SET layers. The active thickness of the silicon is denoted by d_{Si} and that of the support by d_{Sup}.

Layer	R_{In} [mm]	R_{Out} [mm]	Z [mm]	d_{Si} [µm]	d_{Sup} [µm]
SIT 1	165		371	275	1000
SIT 2	309		645	275	1000
SET 1	1833		2350	275	1000
SET 2	1835		2350	275	1000
ETD 1	419	1823	2426	275	1000
ETD 2	419	1823	2428	275	1000
ETD 3	419	1823	2430	275	1000

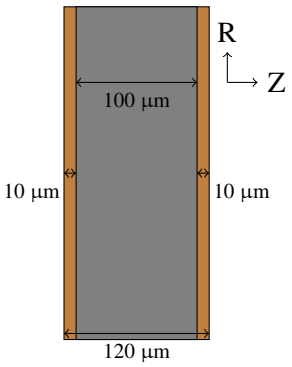

Figure 4: Layout of the TPC cathode, as implemented in the simulation.

Table 5: TPC parameters

Parameter	Value
Half-Length	2350 mm
Inner Radius	329 mm
Outer Radius	1808 mm
Cage Material	Aluminium
Gas	Ar,CO_2,CH_4
Endplate	28.1% X_0
Number of Pad rows	224

3.5. Silicon Envelope: ETD and SET

Another layer of silicon detectors is placed around the TPC. These are the Endcap Tracking Disks (ETDs), located between the TPC endplate and the ECal endcap, and the Silicon External Tracker (SET), surrounding the outer barrel of the TPC field cage. The ETDs consist of three strip layers with stereo angles and the SETs of two layers. The parameters for these devices can be found in Table 4.

3.6. Material Budget, Sensor Coverage and Resolution of the Tracking Detectors

3.6.1. Material Budget

The material budget in the simulation is shown in Figure 5. It shows that the total amount of material in the vertex detector, including the beryllium support, is less than 2% of a radiation

length (X_0).

The material before the ECal amounts to less than 10% X_0 in the barrel. There is more material before the ECal endcap, because of the TPC endplate with a thickness of 28% X_0.

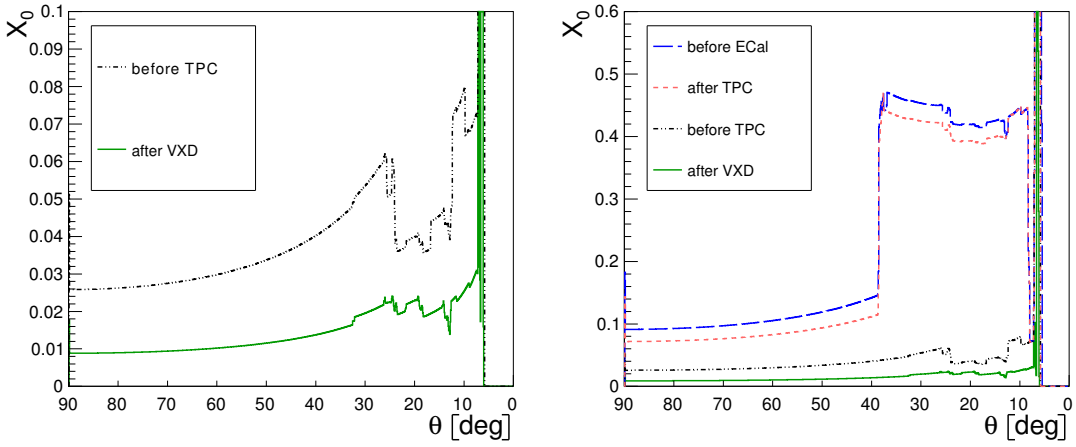

(a) (b)

Figure 5: The radiation length X_0 in the tracking detectors, including the beam pipe, with respect to the polar angle θ. The conical beam pipe causes the peak at $\theta \approx 7^\circ$ (see Subsection 6.3).

3.6.2. Sensor Coverage

The coverage of the tracking detectors with respect to the polar angle is shown in Figure 6. In the barrel all six vertex and two SIT layers are traversed by the particles before they pass through the TPC. At 30°, where the TPC coverage is diminished, the forward tracking disks start to take over the tracking.

3.6.3. Single Hit Resolution

The simulation does not contain parameters on the pixel or strip size of the tracking detectors. This information is used only during the digitization and reconstruction stage to smear the position of the energy deposits recorded during the simulation. Table 6 provides the assumed resolutions for the different tracking detectors. The resolution for the ETDs is obtained from the combination of all three strip layers.

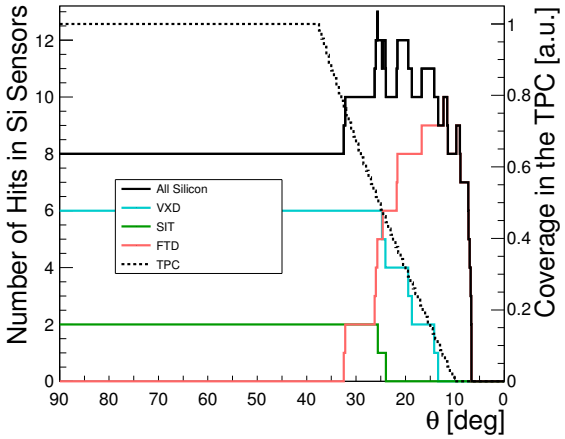

Figure 6: Number of hits in the silicon detectors and fraction of TPC pad rows covered with respect to the polar angle θ. ETD and SET are neither shown nor included in "All Silicon".

Table 6: Single hit resolutions for all tracking detectors, as used for the digitization done after the simulation. For the TPC, the resolution depends on the position of the Hit.

Detector Type	$\sigma_{R\phi}$ [μm]	σ_R [μm]	σ_Z [μm]
Vertex Barrel	2.8		2.8
SIT	7.0		50.0
SET	7.0		50.0
TPC	A		B
Vertex Endcap	2.8	2.8	
FTD	7.0	50.0	
Combined ETD	7.0	7.0	

A $\sqrt{(50\ \mu\text{m})^2 + (53\ \mu\text{m})^2 \cdot Z_{\text{Drift}}/\text{m} \cdot \sin\vartheta + (900\ \mu\text{m})^2/\sin^2\beta}$

B $\sqrt{(400\ \mu\text{m})^2 + (800\ \mu\text{m})^2 \cdot Z_{\text{Drift}}/\text{m})}$

Z_{Drift} is the driftlength from energy deposit to endplate, θ is the polar angle, and β is the angle of the helix relative to the pad row.

4. Calorimeters

4.1. Electromagnetic Calorimeter (ECal)

The ECal is a high granularity sampling calorimeter with tungsten absorber layers and sensitive silicon elements. A detailed description of the layer structure can be found in references [2, 3]. Both the ECal barrel and endcap consist of 29 layers. The first 20 tungsten absorber layers are 2.1 mm thick, the last nine absorber layers are 4.2 mm thick. The gap for the sensors between

two tungsten plates is 3.15 mm and the cell size for the active elements is about 5×5 mm^2. The silicon is 0.5 mm thick, the gap is also filled by material representing support and electronics. The depth of the electromagnetic calorimeter is about 23 X_0 and slightly more than 1 λ_I (see Figure 7).

4.2. Hadronic Calorimeter (HCal)

The hadronic calorimeter consists of two different absorber types. In the barrel 10 mm thick tungsten layers are used. In the endcap 20 mm iron plates are the absorber. The tungsten is a mixture of 93% tungsten, 6.1% nickel and 0.9% iron. The performance of different absorber thicknesses and materials is discussed in [4]. In both parts the gap for the sensitive layer is 6.5 mm. The polystyrene scintillator in the gap is 5 mm thick with a tile size of 30×30 mm^2. More details on the structure of the active layers and of the HCal in general can be found in reference [5].

Both, the endcap and the barrel, are around 8 λ_I deep, which brings the total thickness of the calorimeters to 9 λ_I (see Figure 7).

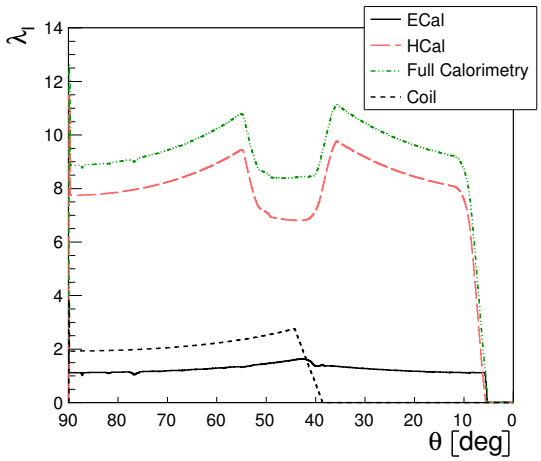

Figure 7: Nuclear interaction lengths λ_I in the calorimeters and coil with respect to the polar angle θ.

4.3. Instrumented Yoke

The whole detector is surrounded by an iron return yoke to limit magnetic stray fields. The iron is interspersed with layers of RPCs, that are used for muon identification and can act as a tail catcher. Because of the approximately 2 λ_I in the coil, the muon system in the barrel starts with an active layer. In the endcap the first layer of the muon system follows the first 150 mm of iron in the yoke plug.

In the simulation, both the endcap and the barrel are made of 18 layers of 100 mm absorber and 40 mm gaps for the RPCs. For the reconstruction, however, only three groups of three of

Table 7: Parameters for the calorimeter layers. The number of layers N_{Layers}, the thickness of one layer d_{Layer}, the absorber material, its thickness d_{Abs}, the active material and its thickness d_{Act} is given.

	N_{Layers}	d_{Layer} [mm]	Absorber	d_{Abs} [mm]	Active	d_{Act} [mm]
ECal 1	20	5.25	Tungsten	2.1	Silicon	0.50
ECal 2	9	7.35	Tungsten	4.2	Silicon	0.50
HCal Barrel	75	16.50	Tungsten	10.0	Scintillator	5.00
HCal Endcap	60	26.50	Iron	20.0	Scintillator	5.00

those layers are used. These groups are: 1, 2 and 3; 8, 9 and 10; 15, 16 and 17. For the endcap the layer inside the yoke plug is used additionally. The muon system is described in [6].

5. Solenoid and Magnetic Field

The coil is implemented as an aluminium cylinder with the parameters given in Table 1. The dimensions include the size of the cryostat. The material is about 2 λ_{I} thick. The magnetic field in the simulation is a pure solenoid field of 4 T parallel to the detector axis. The field in the return yoke barrel is 1.5 T and pointing in the opposite direction. The field switches in the centre of the solenoid coil at $R = 3750$ mm. There is no field beyond the end of the coil at $|Z| = 4256$ mm, which means there is no field simulated in the yoke endcap (see Table 8).

Table 8: Geometrical parameters for the magnetic field. R_{Max} is the outer radius of the magnetic field and Z_{Max} is the extent of the field parallel to the beam axis.

	B_{Z} [T]	R_{Max} [mm]	Z_{Max} [mm]
Solenoid	4.0	3750	4256
Yoke	-1.5	6945	4256

6. Forward Calorimeters, Beam Pipe and other components

6.1. Luminosity Calorimeter (LumiCal)

The main purpose of the LumiCal is the precise measurement of electrons and positrons from Bhabha events. It consists of 40 layers of 3.5 mm tungsten and 0.32 mm silicon sensors. Each layer also contains 0.2 mm support (consisting of epoxy, kapton and copper) and 0.25 mm air gaps (see Table 9). The position and size of the LumiCal provide an overlap of the coverage between itself and the ECal endcap (see Table 1). A detailed study of the performance of the LumiCal at CLIC can be found in reference [7].

Table 9: Parameters of the forward calorimeter layer structure. The number of layers N_{Layers}, their thickness d_{Layer}, the absorber material, its thickness d_{Abs}, the active material and its thickness d_{Act} is given.

	N_{Layers}	d_{Layer} [mm]	Absorber	d_{Abs} [mm]	Active	d_{Act} [mm]
LumiCal	40	4.27	Tungsten	3.5	Silicon	0.32
BeamCal	40	4.00	Tungsten	3.5	Diamond	0.30

6.2. Beam Calorimeter (BeamCal)

The BeamCal completes the coverage of the electromagnetic calorimeter down to 10 mrad (see Table 1). Like the LumiCal, the BeamCal consists of 40 layers of 3.5 mm tungsten plates. But the sensor material has to be radiation hard, because the BeamCal has to absorb a large part of the incoherent electron-positron pairs from the beam-beam interaction. In the simulation 0.3 mm thick diamond layers are used for the active elements. To reduce the amount of particles scattering back into the detector, the IP-facing side of the BeamCal is covered with a 100 mm thick graphite layer.

6.3. Beam Pipe

The geometrical parameters of the different parts of the beam pipe are described in Table 10 and the beam pipe can be seen in Figure 2 and Figure 8.

Around the interaction point the beam pipe consists of a beryllium cylinder. Because of the specific radius and length of the cylinder, the complete angular coverage of the tracking detectors is covered by this cylinder.

The next part of the beam pipe is an iron cone with a half-opening of $\approx 7^\circ$. The wall thickness of this cone is 4 mm to absorb particles scattering back from the forward region [8]. The maximal cone radius is given by the inner radius of the ECal endcap. At a radius of 240 mm the beam pipe becomes cylindrical until the front face of the LumiCal.

Inside the LumiCal the beam pipe is aligned with the outgoing beam axis, and the radius is limited by the inner radius of the LumiCal. The beam pipe changes again before the BeamCal, when it splits into two separate pipes: A thin cylindrical beam pipe for the incoming beam, and a conical beam pipe with a half-opening angle of 10 mrad for the outgoing beam.

6.4. Support Tube and Accelerator Components

Some additional components, shown in Figure 8, are approximated by cylinder barrels in the simulation. Placed close to the beam pipe are the Kicker and Beam Position Monitor (BPM) of the intra-train feedback and the permanent-magnet core of the final focus quadrupole QD0. Around the beam pipe and the pieces in the very forward region sits a support tube, that extends up to the LumiCal. Inside the yoke plug and endcap sits an anti-solenoid, which is aligned with the core of the QD0.

Table 10: Parameters for the beam pipe parts. Each part is a cylinder barrel or cone positioned between Z_1 to Z_2, the radii $R_{1/2}^{\mathrm{In/Out}}$ are the inner and outer radii at position $Z_{1/2}$ respectively.

&[A]	Z_1 [mm]	Z_2 [mm]	R_1^{In} [mm]	R_2^{In} [mm]	R_1^{Out} [mm]	R_2^{Out} [mm]	Material
0	0	260	29.4	29.4	30.0	30.0	Be
0	260	289	29.4	29.4	30.0	33.4	Iron
0	289	2080	29.4	235.2	33.4	240.0	Iron
0	2080	2645	235.2	235.2	240.0	240.0	Iron
0[B]	2645	2646	0.0	98.0	240.0	240.0	Iron
2	2646	3170	98.0	98.0	99.0	99.0	Iron
2[C]	3170	3171	2.7	31.0	99.0	99.0	Iron
2	3171	3500	31.0	31.0	32.0	32.0	Iron
2[D]	3500		31.0		32.0		Iron
1	3171	12500	2.7	2.7	3.7	3.7	Iron

[A] Alignment of beam-pipe part: 0 (aligned on detector axis), 1 (aligned on incoming-beam axis), 2 (aligned on outgoing-beam axis).

[B] Beam-pipe end in front of LumiCal: R_1^{Out} is the size of the hole where the beam pipe inside LumiCal is connected. The hole is centred on the outgoing beam axis.

[C] Beam-pipe end in front of BeamCal: R_1^{In} is the size of the hole for the incoming beam pipe, R_1^{Out} is the size of the hole for the outgoing beam pipe.

[D] Conical beam pipe with an half-opening angle of 10 mrad.

Table 11: Geometrical parameters for the mask and accelerator components in the simulation

	Z_1 [mm]	Z_2 [mm]	R_{In} [mm]	R_{Out} [mm]	Material
Support Tube	2875	7500	300.0	400	Iron
Beam Position Monitor	3480	3570	35.0	54	Iron
Kicker	3580	3880	4.0	25	Iron
QD0	4256	6965	3.8	35	Iron
Anti-Solenoid	4256	7235	401.0	685	Iron

7. Simulation Software

The CLIC_ILD_CDR model is implemented in the GEANT4-based [9] full detector simulation MOKKA [10]. GEANT4 version 9.3p2 and the QGSP_BERT physics list with a range cut of 0.1 mm are used for the mass production. To account for the crossing angle at the 3 TeV CLIC all particles are boosted by 10 mrad in the horizontal plane.

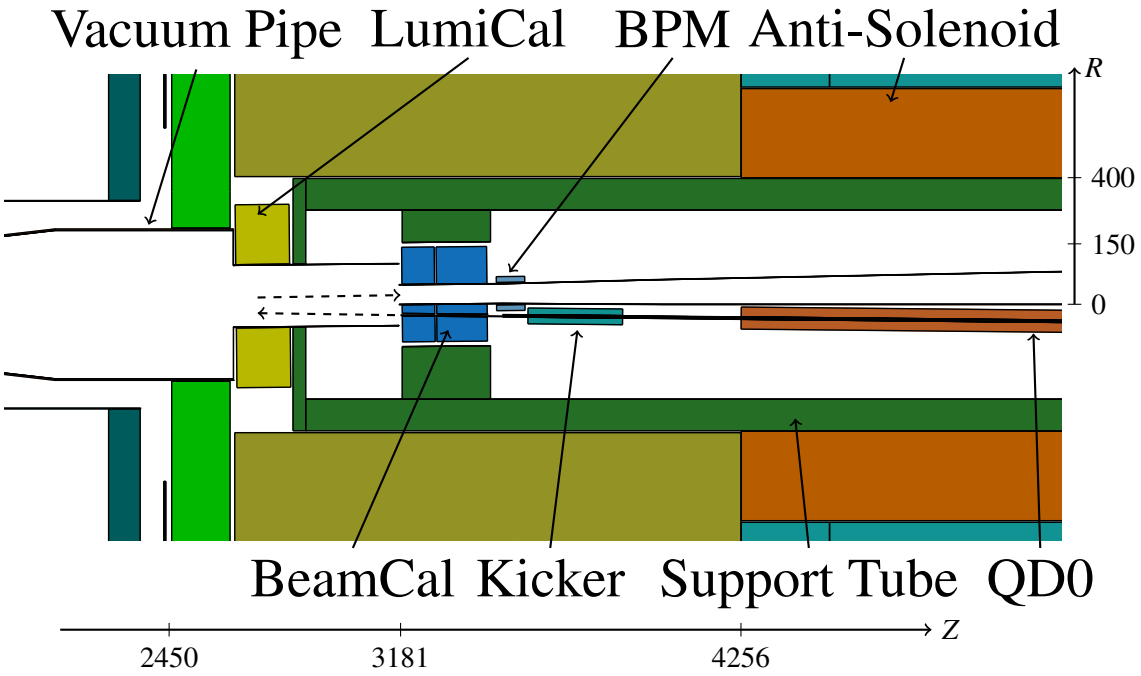

Figure 8: Very forward region with forward calorimeters and some accelerator equipment

References

[1] ILD Concept Group. The International Large Detector Letter of Intent. 2009. DESY-09-087.

[2] The CALICE collaboration. Design and electronics commissioning of the physics prototype of a Si-W electromagnetic calorimeter for the International Linear Collider. *Journal of Instrumentation*, vol. 3(08) p. P08001, 2008. ArXiv:0805.4833v2.

[3] The CALICE collaboration. Response of the CALICE Si-W Electromagnetic Calorimeter Physics Prototype to Electrons, 2009. ArXiv:0811.2354.

[4] P. Speckmayer and C. Grefe. Comparison of performance of hadronic tungsten and steel sampling calorimeters. LCD-Note-2010-001, 2010.

[5] A. Lucaci-Timoce and R. Diener. Description of the HCAL Detector in Mokka. LC-Tool-2008-001, 2008.

[6] E. van der Kraaij and B. Schmidt. Design of the Muon System for the CLIC Detectors. LCD Note in preparation, 2011.

[7] I. Sadeh, H. Abramowicz, R. Ingbir, S. Kananov, and A. Levy. A Luminosity Calorimeter for CLIC. LCD-Note-2009-002, 2009.

[8] D. Dannheim and A. Sailer. Beam-induced backgrounds in the CLIC detectors. LCD-Note-2011-021, 2011.

[9] S. Agostinelli et al. Geant4 – A Simulation Toolkit. *Nucl. Instrum. Methods Phys. Res., Sect. A*, vol. 506(3) pp. 250–303, 2003.

[10] P. Mora de Freitas and H. Videau. Detector Simulation with Mokka/Geant4 : Present and Future. In *International Workshop on Linear Colliders (LCWS 2002)*. JeJu Island, Korea, 2002.

A. Errata and Addenda

A.1. May 11, 2011

- Table 1: The outer radii for all endcap detector pieces in were wrong. Written were the circumscribing radii, and not the inscribing radii as intended.
- Table 5: Added the number of pad rows (224)
- Table 10: Added one significant digit to the radii for the beam pipe parts. Clarified footnote B

A.2. November 24, 2011

- Table 1, Table 5: The TPC half length is 2350 mm, as indicated in Figure 1, and not 2250 mm.
- Table 6: Replaced the resolution given for the TPC by the correct position-dependent resolution terms.
- Figure 8: Added Scales.

A.3. March 15, 2012

- Table 2: Corrected position of outer layers in VXD doublets. They are positioned 67 μm further outwards (XX.933 instead of XX.866)
- Table 3: Corrected outer radius of FTD6 (from 175 mm to 102 mm) and FTD7 (from 302 to 175)

A.4. November 7, 2014

- Subsection A.3: Corrected value of old position of VXD, wrongly written XX.696
- Table 7: Corrected absorber thickness for second part of the ECal from 4.1 mm to 4.2 mm

A.5. November 25, 2014

- Table 7: Corrected total layer thickness d_{Layer} for the ECal to be consistent with the text and to correct ECal 2 thickness:
  - Give two significant digits. Changed $d_{\text{Layer}}^{\text{ECal1}}$ from 5.3 mm to 5.25 mm
  - Corrected $d_{\text{Layer}}^{\text{ECal2}}$ from 7.3 mm to 7.35 mm, accounting for corrected absorber thickness in previous erratum.